Ionics
https://doi.org/10.1007/s11581-019-03301-0

BRIEF COMMUNICATION

Enhanced thermal decomposition performance of sodium perchlorate by molecular assembly strategy

Peng Deng[1,2] · Hui Ren[1] · Qingjie Jiao[1]

Received: 17 August 2019 / Revised: 26 September 2019 / Accepted: 6 October 2019

Abstract

$NaClO_4$-based molecular perovskite $(H_2dabco)[Na(ClO_4)_3]$ combined with the inorganic oxidizer and organic fuel was prepared by molecular assembly strategy. The high-yield samples were obtained by the one-pot reaction of $NaClO_4$, $HClO_4$, and triethylenediamine (dabco). The thermal analysis results showed molecular perovskite $(H_2dabco)[Na(ClO_4)_3]$ with ABX_3-type closely ternary molecular stacking structure had a lower decomposition temperature (381.7 °C) and a higher heat release (2770 J/g) than $NaClO_4$ (569.2 °C and 353 J/g). The apparent activation energy of thermal decomposition process was reduced by 25 kJ/mol from 184.8 kJ/mol of $NaClO_4$ to 159.8 kJ/mol of $(H_2dabco)[Na(ClO_4)_3]$. A synergistic catalysis thermal decomposition mechanism was proposed. The H_2dabco^{2+} from the unique ternary molecular perovskite structure can be favorable for proton excitation under thermal stimuli, and promote the formation of $HClO_4$ and superoxide radical anions $\cdot O_2^-$ further, resulted in the redox thermal decomposition reaction between oxidizer ClO_4^- and fuel dabco more completely.

Keywords Organic-inorganic · Fuel · $(H_2dabco)[Na(ClO_4)_3]$ · Molecular perovskite · Thermal decomposition performance

Introduction

As a primary class of high-energy solid oxidizers, $NaClO_4$ has received much attention in the fields of the propellants, explosives, and pyrotechnics [1–3]. Current studies mainly aimed at increasing the thermal decomposition performance of $NaClO_4$. Reducing the thermal decomposition temperature, decreasing the reaction activation energy, and enhancing the decomposition heat release are benefit for a shorter ignition delay time and a higher burning rate [4–7]. It is significant to promote their applications in modern military and industrial fields.

To date, main research works have been reported for the decomposition energy release of $NaClO_4$-based composites by nano-metal and its oxides introduced [8–11]. But, many inevitable disadvantages were brought, such as low heat release, high thermal decomposition temperature, high ignition threshold, high cost, and complicated fabrication process, which limited its potential application on a deeper level severely [12–15]. Therefore, development of high-performance $NaClO_4$-based energetic materials is urgent and necessary to meet its requirements.

Molecular assembly structures with novel and unique properties have much attention and have many applications in the scientific fields [16–25]. Especially in energetic materials, combined with the high-energy inorganic oxidizer and organic fuel at the molecular level, the molecular assembly strategy was pioneered by Chen's group [26]. The high-symmetry ternary molecular perovskite with advanced properties can be constructed by a facile and simple method. It is important to study the thermal decomposition performance of $NaClO_4$-based molecular perovskite. And it is also essential to understand their thermal decomposition behavior and thermodynamics for the future applications.

In this work, $NaClO_4$-based molecular perovskite $(H_2dabco)[Na(ClO_4)_3]$ was prepared by molecular assembly strategy. The chemical structure was characterized and the thermal decomposition behavior and thermodynamics were investigated. And the synergistic catalysis thermal decomposition mechanism was proposed based on the unique ternary organic-inorganic hybrid molecular perovskite structure.

✉ Hui Ren
renhui@bit.edu.cn

[1] State Key Laboratory of Explosion Science and Technology, Beijing Institute of Technology, Beijing 100081, China

[2] School of Environment and Safety Engineering, North University of China, Taiyuan 030051, China

Published online: 08 November 2019

Experimental

Materials and method

$NaClO_4$ microparticle materials and perchloric acid (H_2O solution, 70%) were provided from Shanxi Jiangyang Chem. Eng. Co., Ltd. Triethylenediamine (1,4-diazabicyclo[2.2.2]octane, dabco) was provided by Shanghai Aladdin Biochemical Technology Co., Ltd. Deionized water was made in laboratory.

0.1 mmol $NaClO_4$, 0.1 mmol dabco, and 0.163 ml $HClO_4$ solution were added into beaker with 20 ml deionized water, and solid particles were dissolved completely at 25 °C for 1 h. The matrix was transferred to the room to crystallize naturally. After a week, the white crystal samples were collected by filtration, washing, and drying. The yield of the product is over 90%.

Characterization

X-ray diffraction (XRD) pattern of as-obtained sample was collected on a Philips X'Pert Pro X-ray diffractometer (PANalytical, Holland) by Cu-Kα radiation. Fourier transform infrared (FT-IR) spectrums were obtained on a Thermo Scientific Nicolet iS 50 spectrophotometer (Thermo Scientific, USA). The thermal decomposition process were detected by a STA449F3 thermogravimetric-differential scanning calorimeter (Netzsch, Germany) with the different heating rates (5, 10, 15, and 20 °C/min) in a N_2 atmosphere over the temperature ranged from 50 to 1000 °C.

Results and discussion

Figure 1a shows the XRD patterns of as-prepared $NaClO_4$-based molecular perovskite samples. The diffraction peaks at 12.57°, 21.75°, 28.21°, and 38.10° corresponded to the crystal planes (200), (222), (420), and (600), respectively, which is in great agreement with its simulated powder XRD pattern (CCDC: 1528106). Other peaks were unapparent because of the lower exposure probabilities of those crystal planes. From the literatures [27, 28], the structure of $(H_2dabco)[Na(ClO_4)_3]$ belongs to the ABX_3-type molecular perovskite. Protonated H_2dabco^{2+} cation was considered the A-site cation in this system, Na^+ cation as the B-site cation, and ClO_4^- anion as the X-bridges. Figure 1b shows the schematic of perovskite structure. Each Na^+ cation on the corners, face, and body centers of the cubic perovskite structure is coordinated with twelve oxygen atoms from six ClO_4^- anions by noncovalent bonds. And each ClO_4^- anion can be considered X-bridges ligand, resulted in the formation of the three-dimensional anionic cage–like frameworks. Protonated H_2dabco^{2+} cations are embedded and locked in three-dimensional anionic cage–like frameworks to balance the overall charge. The strong Coulomb interactions between anions and cations, hydrogen bonds and so on, lead to the high stability of ternary organic-inorganic hybrid perovskite structure.

The FT-IR spectra of the samples are shown in Fig. 2. The key groups of organic-inorganic hybrid molecular perovskite $(H_2dabco)[Na(ClO_4)_3]$ located at 1070 cm^{-1} corresponded to the oxidant group ClO_4^- anions. The peaks at 1050, 891, and 847 cm^{-1} originated from skeletal motion of protonated H_2dabco^{2+} cations. Compared with the component dabco, the red shift of C-H vibrational bonds ranged from 3000 to 3300 cm^{-1} of protonated H_2dabco^{2+} occurred because of the formation of hydrogen bonds from H atoms of protonated H_2dabco^{2+} cations to O atoms of ClO_4^- anions. Combined with XRD and FT-IR results, the organic-inorganic hybrid molecular perovskite $(H_2dabco)[Na(ClO_4)_3]$ can be fabricated by molecular assembly strategy.

Figure 3 shows the thermal decomposition process of the samples by DSC tested. In Fig. 3a, the main peaks of component $NaClO_4$ at 309.2, 472.3, 569.2, 801.0, and 814.0 °C can be observed. The thermal decomposition of $NaClO_4$ was divided into two stages. In the first decomposition stage, the endothermic peak at 309.2 and 472.3 °C is ascribed to the crystallographic transition from orthorhombic to cubic and melting process of $NaClO_4$, respectively. The exothermic peak at 569.2 °C corresponded to thermal decomposition of

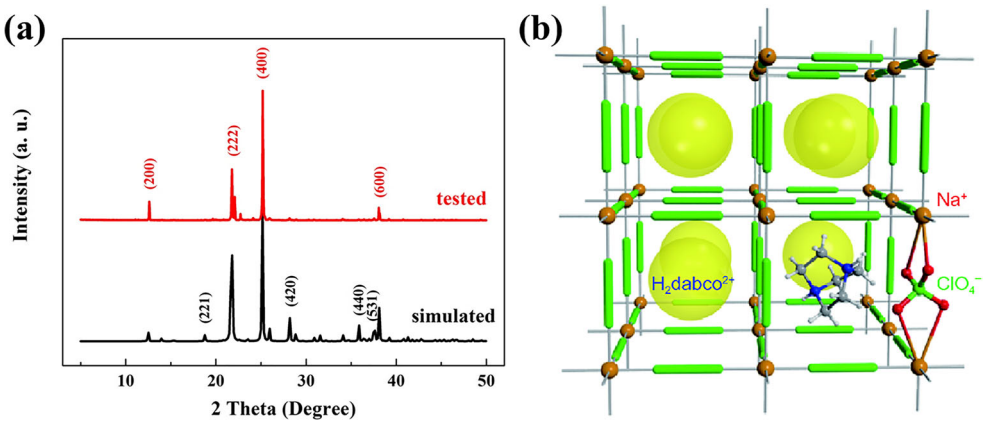

Fig. 1 **a** XRD patterns and **b** schematic [26] of perovskite structure of $(H_2dabco)[Na(ClO_4)_3]$

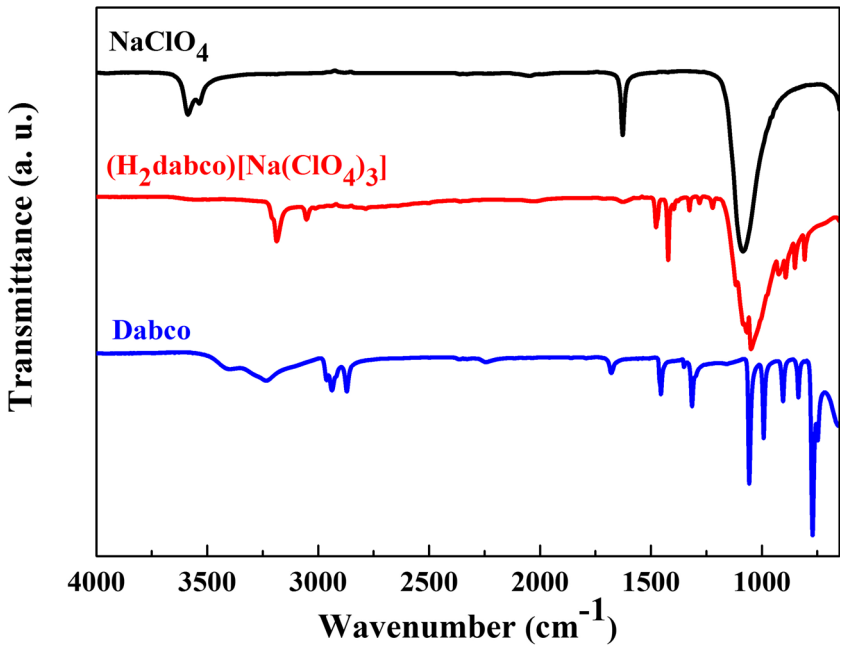

Fig. 2 FT-IR spectra of samples: $NaClO_4$, dabco, and $(H_2dabco)[Na(ClO_4)_3]$

$NaClO_4$. The heat release of primary thermal decomposition stage is 353 J/g. And the second stage demonstrated melting and decomposition processes of intermediate product NaCl. For $(H_2dabco)[Na(ClO_4)_3]$, the main decomposition peaks appeared at 207.9 and 381.7 °C can be ascribed to structure change endothermic processes of ring skeleton of A-site protonated H_2dabco^{2+} cations and thermal decomposition of $(H_2dabco)[Na(ClO_4)_3]$ [29]. Compared with the monocomponent $NaClO_4$, the exothermic peak temperature (381.7 °C) of $(H_2dabco)[Na(ClO_4)_3]$ had been reduced greatly by 187.5 °C. The decomposition heat had increased up to 2770 J/g, which was about as eight times as that of $NaClO_4$. That revealed hybrid molecular perovskite $(H_2dabco)[K(ClO_4)_3$ combined with the inorganic oxidizer $NaClO_4$ and organic fuel dabco can produce more heat by reaction with each other. Especially, during the decomposition process of $NaClO_4$, phase transition and melting required absorbing enough heat energy from the system, which is not benefit for the improvement of heat release. Integrated with oxidizer and fuel in a molecular perovskite cell, low thermal decomposition temperature and high heat release from the novel hybrid perovskite structure can provide more ways towards the potential applications of $NaClO_4$.

The thermal decomposition dynamics of as-obtained samples were studied further by DSC. As shown in Fig. 4 a and b, the DSC curves at the different heat rates were collected. The kinetic parameters of thermal decomposition of samples were calculated by the Kissinger equation in Fig. 4 [30]. The reaction activation energy (E_a) of $(H_2dabco)[Na(ClO_4)_3]$ thermal decomposition was calculated to be 159.8 kJ/mol, which is lower than $NaClO_4$ (184.8 kJ/mol). That revealed the ternary organic-inorganic hybrid molecular perovskite $(H_2dabco)[Na(ClO_4)_3]$ is easier to be activated under the thermal stimuli.

Combined with the experiments and results, the synergistic catalysis thermal decomposition mechanism was proposed based on the unique ternary organic-inorganic hybrid molecular perovskite structure. As shown in Fig. 5, Organic fuel small molecule protonated H_2dabco^{2+} cations in the ternary system can be activated easily at lower temperature, but were

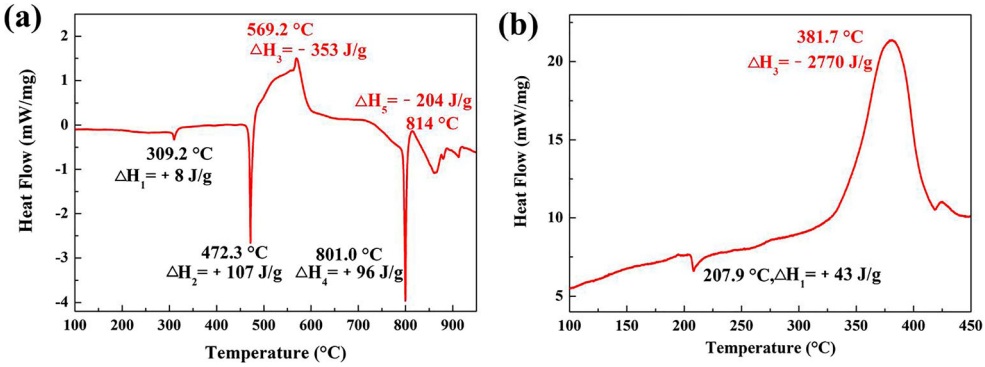

Fig. 3 DSC curves of **a** $NaClO_4$ and **b** $(H_2dabco)[Na(ClO_4)_3]$

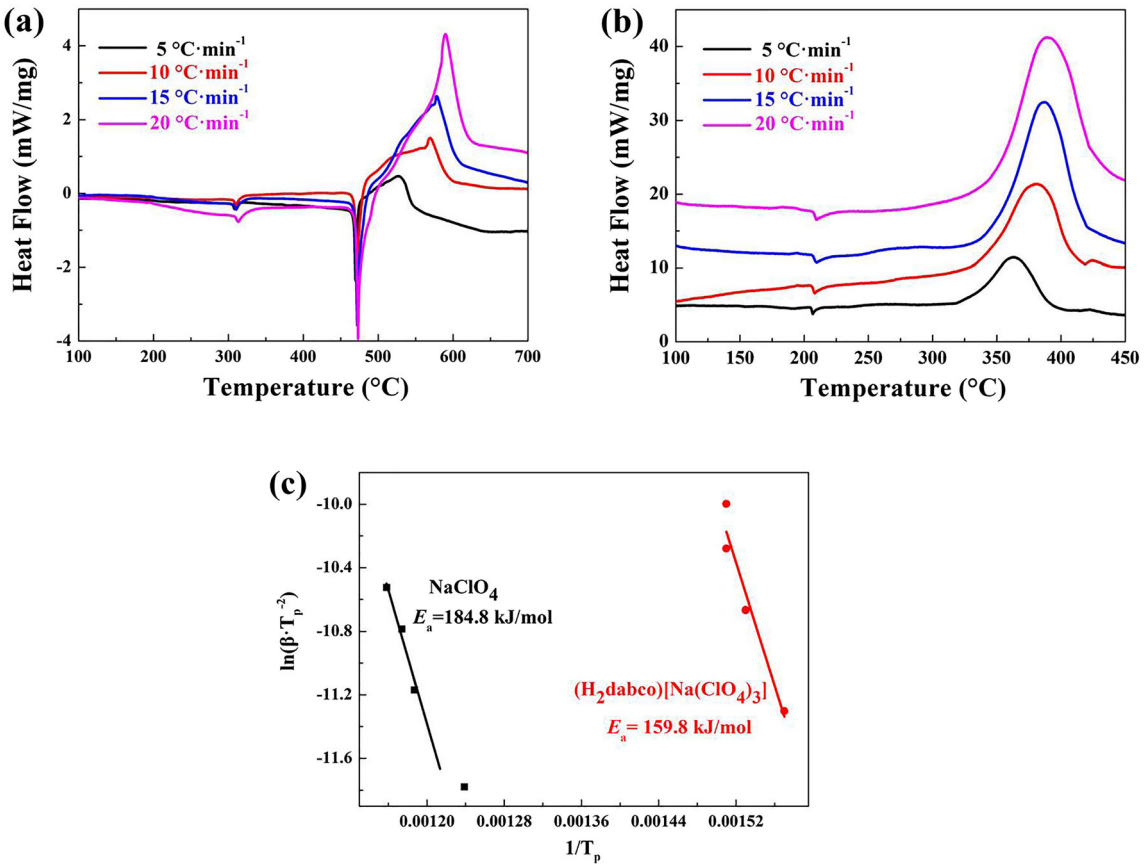

Fig. 4 DSC curves of **a** $NaClO_4$ and **b** $(H_2dabco)[Na(ClO_4)_3]$ at different heating rates. **c** Dependence of $\ln(\beta/T_p^2)$ versus $1/T_p$. Scatter points are experimental data and line denotes the linear fitting results

still locked in the three-dimensional anionic cage–like frameworks rather than escaping due to the space hindered effect [29]. When heating energy becomes greater than the Coulomb forces of anionic frameworks, the cage-like frameworks were destroyed. And many activated protonated H_2dabco^{2+} cations can render protons quickly and facilitate proton transfer from H_2dabco^{2+} to ClO_4^-, resulting in the formation of $HClO_4$ as well as superoxide radical anions $\cdot O_2^-$ further. The organic fuel dabco will react with $\cdot O_2^-$ subsequently, resulted in the redox thermal decomposition reaction between oxidizer ClO_4^- and fuel dabco more completely, and more decomposition heat was released. Organic-inorganic hybrid molecular perovskite $(H_2dabco)[Na(ClO_4)_3]$ combined with the high-energy oxidizer and fuel can not only reduce the thermal decomposition temperature and enhance the heat release, but also decrease E_a of thermal decomposition, which offers a

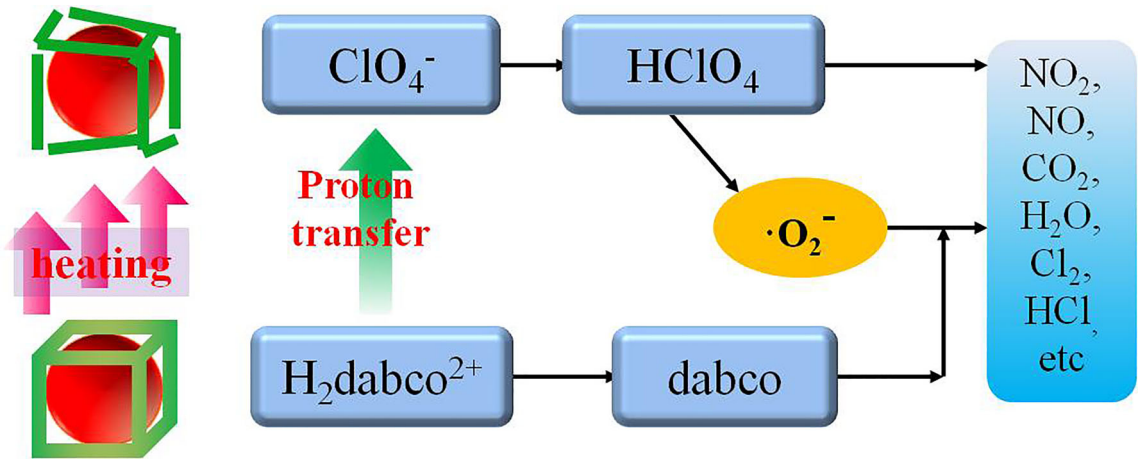

Fig. 5 Schematic of the thermal decomposition of $(H_2dabco)[Na(ClO_4)_3]$

potential application prospect in the explosives and propellant fields.

Conclusions

In summary, the ternary organic-inorganic hybrid molecular perovskite $(H_2dabco)[Na(ClO_4)_3]$ was prepared successfully by the molecular assembly strategy. The yield of product is over 90% by the facile one-pot reaction. And thermal analysis results showed $(H_2dabco)[Na(ClO_4)_3]$ with hybrid molecular perovskite structure had a lower decomposition temperature (381.7 °C) than $NaClO_4$ (569.2 °C). The high heat release (2770 J/g) which is about seven times higher than the monocomponent $NaClO_4$ (353 J/g) was originated from the molecular perovskite structure combined with the high-energy oxidizer $NaClO_4$ and fuel dabco. Moreover, the E_a of $(H_2dabco)[Na(ClO_4)_3]$ (159.8 kJ/mol) becomes lower, compared with $NaClO_4$ (184.8 kJ/mol). The synergistic catalysis thermal decomposition mechanism of $(H_2dabco)[Na(ClO_4)_3]$ was proposed based on the unique hybrid molecular perovskite structure.

Acknowledgments The authors thank Prof. Weixiong Zhang and Dr. Shaoli Chen (Sun Yat-sen University, Guangzhou, China) for support and help.

Funding information This work was supported by the Natural Science Foundation of China (21975024 and 11372290).

Compliance with ethical standards

Conflict of interest The authors declare that they have no conflict of interest.

References

1. He W, Liu P, He G, Gozin M, Yan QL (2018) Highly reactive metastable intermixed composites (MICs): preparation and characterization. Adv Mater 30:e1706293. https://doi.org/10.1002/adma.201706293
2. Chen J, He S, Huang B, Wu P, Qiao Z, Wang J, Zhang L, Yang G, Huang H (2017) Enhanced thermal decomposition properties of CL-20 through space-confining in three-dimensional hierarchically ordered porous carbon. ACS Appl Mater Interfaces 9:10684–10691. https://doi.org/10.1021/acsami.7b00287
3. Deng P, Liu Y, Luo P et al (2017) Two-steps synthesis of sandwich-like graphene oxide/LLM-105 nanoenergetic composites using functionalized graphene. Mater. Lett. 194:156–159. https://doi.org/10.1016/j.matlet.2017.02.038
4. Li Q, He Y, Peng R (2015) Graphitic carbon nitride (g-C3N4) as a metal-free catalyst for thermal decomposition of ammonium perchlorate. RSC Adv 5:24507–24512. https://doi.org/10.1039/C5RA01157D
5. Cao X, Deng P, Hu S et al (2018) Fabrication and characterization of nanoenergetic hollow spherical hexanitrostibene (HNS) derivatives. Nanomaterials 8:336. https://doi.org/10.3390/nano8050336
6. Thiruvengadathan R, Chung S, Basuray S, Balasubramanian B, Staley CS, Gangopadhyay K, Gangopadhyay S (2014) A versatile self-assembly approach toward high performance nanoenergetic composite using functionalized graphene. Langmuir 30:6556–6564. https://doi.org/10.1021/la500573e
7. Cao X, Shang Y, Meng K et al (2019) Fabrication of three-dimensional TKX-50 network-like nanostructures by liquid nitrogen-assisted spray freeze-drying method. J Energ Mater 37:356–364. https://doi.org/10.1080/07370652.2019.1585491
8. Chakravarty A, Bhowmik K, Mukherjee A, de G (2015) Cu_2O nanoparticles anchored on amine-functionalized graphite nanosheet: a potential reusable catalyst. Langmuir 31:5210–5219. https://doi.org/10.1021/acs.langmuir.5b00970
9. Intaphong P, Radklaochotsatain N, Somraksa W et al (2019) Combustion synthesis of nickel ferrite powders: effect of $NaClO_4$ content on their characteristics and magnetic properties. Curr. Appl. Phys. 19:548–555. https://doi.org/10.1016/j.cap.2019.02.006
10. Terashima Y, Takeda K, Honda M (2011) Phase behaviour and molecular dynamics in the binary system of sodium perchlorate and 1,2-propanediamine. J Chem Thermodyn 43:307–310. https://doi.org/10.1016/j.jct.2010.09.011
11. Busurin S, Busurina M, Kuznetsov M et al (2010) Thermolysis in the BaO_2–$NaClO_4$ System. Dokl Phys Chem 431:772–777. https://doi.org/10.1134/S0012501610040068
12. Elbasuney S, Fahd A (2019) Combustion wave of metalized extruded double-base propellants. Fuel 237:1274–1280. https://doi.org/10.1016/j.fuel.2018.10.018
13. Chen W, Chang L, Ren S et al (2019) Direct Z-scheme 1D/2D WO2.72/ZnIn2S4 hybrid photocatalysts with highly-efficient visible-light-driven photodegradation towards tetracycline hydrochloride removal. J Hazard Mater. https://doi.org/10.1016/j.jhazmat.2019.121308
14. Deng P, Xu J, Li S et al (2018) A facile one-pot synthesis of monodisperse hollow hexanitrostilbene-piperazine compound microspheres. Mater Lett 214:45–49. https://doi.org/10.1016/j.matlet.2017.11.104
15. Boldyrev V (2006) Thermal decomposition of ammonium perchlorate. Thermochim Acta 443:1–36. https://doi.org/10.1016/j.tca.2005.11.038
16. Wang M, Wang Q, Li J et al (2019) Assembly of large-area reduced graphene oxide films for the construction of Z-scheme over single-crystal porous Bi_5O_7I nanosheets. J Colloid Interf Sci 552:651–658
17. Chen W, He Z, Huang G et al (2019) Direct Z-scheme 2D/2D $MnIn_2S_4$/g-C_3N_4 architectures with highly efficient photocatalytic activities towards treatment of pharmaceutical wastewater and hydrogen evolution. Chem Eng J 359:244–253. https://doi.org/10.1016/j.cej.2018.11.141
18. Li X, Xiong J, Huang J et al (2019) Novel g-C_3N_4/h′$ZnTiO_3$-a′TiO_2 direct Z-scheme heterojunction with significantly enhanced visible-light photocatalytic activity. J Alloy Compd. 774:768–778. https://doi.org/10.1016/j.jallcom.2018.10.034
19. Wang S, He F, Zhao X et al (2019) Phosphorous doped carbon nitride nanobelts for photodegradation of emerging contaminants and hydrogen evolution. Appl Catal B: Environ 257:117931. https://doi.org/10.1016/j.apcatb.2019.117931
20. Wang Y, Wu Z, Weng H et al (2019) Separation of Re(VII) from aqueous solution by acetone-enhanced photoreduction: an insight into the role of acetone. J Photoch Photobio A. 380:111823. https://doi.org/10.1016/j.jphotochem.2019.04.034
21. Yu H, Dong F, Li B et al (2019) Co(II) triggered radical reaction between SO_2 and o-phenylenediamine for highly selective visual colorimetric detection of SO_2 gas and its derivatives. Sensor Actuat B: Chem 299:126983. https://doi.org/10.1016/j.snb.2019.126983
22. Li R, Wang J, He Y et al (2019) Mechanochemical synthesis of defective molybdenum trioxide, titanium dioxide, and zinc oxide

at room temperature. ACS Sustainable Chem Eng 714:11985–11989. https://doi.org/10.1021/acssuschemeng.9b00374
23. Lei J, Guo Q, Yin D et al (2019) Bioconcentration and bioassembly of N/S co-doped carbon with excellent stability for supercapacitors. Appl Surf Sci. 488:316–325. https://doi.org/10.1016/j.apsusc.2019.05.136
24. He Y, Xu B, Li W, Yu H (2015) Silver nanoparticle-based chemiluminescent sensor array for pesticide discrimination. J Agric Food Chem 63:2930–2934. https://doi.org/10.1021/acs.jafc.5b00671
25. Li M, Huang X, Yu H et al (2019) A colorimetric assay for ultrasensitive detection of copper (II) ions based on pH-dependent formation of heavily doped molybdenum oxide nanosheets. Mat Sci Eng C: Mater 101:614–618. https://doi.org/10.1016/j.msec.2019.04.022
26. Chen S, Yang Z, Wang B et al (2018) Molecular perovskite high-energetic materials. Sci China Mater 61:1123–1128. https://doi.org/10.1007/s40843-017-9219-9
27. Deng P, Ren H, Jiao Q (2019) Enhanced the combustion performances of ammonium perchlorate-based energetic molecular perovskite using functionalized graphene. Vacuum 169:108882. https://doi.org/10.1016/j.vacuum.2019.108882
28. Chen S, Shang Y, He C et al (2018) Optimizing the oxygen balance by changing the A-site cations in molecular perovskite high-energetic materials. CrystEngComm 20:7458–7463. https://doi.org/10.1039/c8ce01350k
29. Zhou J, Ding L, Zhao F et al (2019) Thermal studies of novel molecular perovskite energetic material $(C_6H_{14}N_2)[NH_4(ClO_4)_3]$. Chin Chem Lett Accepted. https://doi.org/10.1016/j.cclet.2019.05.008
30. Hu L, Liu L, Hu S et al (2019) 1T/2H multi-phase MoS2 heterostructures: synthesis, characterization and thermal catalysis decomposition of dihydroxylammonium5,5-bistetrazole-1,1-diolate. New J Chem 43:10434–10441. https://doi.org/10.1039/c9nj02749a